Simulation Analysis of Emptying the Explosives in Projectiles with Electromagnetic Heating

Zhiming Qiao [1], Hongjun Xiang [1,*], Genrong Cao [1], Zhibo Qiao [2], Qing'ao Lv [1], Xichao Yuan [1] and Lei Chen [3]

[1] Shijiazhuang Campus, Army Engineering University, Shijiazhuang 050003, China
[2] School of Mechanical Engineering, Hebei University of Technology, Tianjin 300401, China
[3] Key Laboratory of Thermo-Fluid Science and Engineering of MOE, School of Energy & Power Engineering, Xi'an Jiaotong University, Xi'an 710049, China
* Correspondence: xhjyjs@sina.com

Abstract: This paper concerns a new method for projectile disposal by emptying the explosives in projectiles with electromagnetic heating. It explains the basic principles of the emptying technology via electromagnetic heating. A multiphysical analysis model coupled with an electromagnetic, thermal, fluid and phase transition model is established, and the explosive melting simulation is conducted based on this model. The dynamic phase transition process of the explosive from solid to liquid is simulated, and the electric field, magnetic field and thermal field distribution characteristics during the process are analyzed. Furthermore, the effect of excitation current characteristics on the phase transition of the explosive is given, which shows that the explosive melting process is controllable by setting the excitation current amplitude or frequency. This paper provides a new method for the disposal of end-of-life projectiles, which is more controllable, safe and environmentally friendly.

Keywords: projectile disposal; emptying technology; electromagnetic heating; multiphysical simulation

1. Introduction

There are various explosive emptying methods in projectile disposal. The most general method is melting the explosives by heating the projectiles so that the melted explosive flows out. Other methods, such as the cook-off method with flame, boiling method with steam and the soaking method with hot water have been widely applied to heat the projectiles [1–3]. However, there are limitations with these methods applied to melt the explosives. For example, the cook-off method uses flame as a heat source, so it is difficult to control the heating rate, which may easily cause accidents [4,5]. Therefore, it has been gradually abandoned in some countries. The boiling method with steam and the soaking method with hot water produce a large amount of wastewater, which are unfriendly to the environment [6–8]. Since the water pollution problems are not easy to solve, a large amount of manpower and material resources have to be invested to solve the follow-up problems. Therefore, emptying explosives by green harmless disposal ways have gradually become an important issue in projectile disposal research [9].

Emptying explosives with electromagnetic heating is a new method for projectile disposal [10]. In the electromagnetic heating process, the metal projectile shell is placed in a changing magnetic field, and the eddy current occurs according to Faraday's Law, so heat is generated in the shell with the eddy current and then it is transferred to the explosive, which causes the melting of the explosive. This method uses electrical energy as power, so it is a clean way to empty explosives, and the heating rate can be controlled precisely with electrical equipment, so accidents caused by excessive heating rates will be avoided, as will water pollution.

Many scholars have carried out research on heat exchange, induction heating and phase transition, with research results [11–14]. However, the emptying process with the electromagnetic heating method is affected by multiple physical phenomena, such as

electromagnetic fields, thermal fields, hydrodynamics and phase transitions, so it is difficult to describe the process with analytical methods accurately. Therefore, the FEM method is adopted for the numerical simulation of the emptying process in this paper. To study the phenomenon during the phase transition, some researchers have conducted simulation research on typical materials, showing the phase transition process and summarizing the law of typical materials, such as paraffin wax [15–17]. Some researchers have developed models coupled with electric fields, magnetic fields and thermal fields, which show the distribution of various physical fields during the electromagnetic heating process [18–20].

However, multiphysical simulation research on emptying explosives with the electromagnetic heating method has not been reported. In this paper, a multiple physical fields simulation model is developed, and the dynamic emptying process is simulated. It introduces the characteristics of a multiphysical field during the process and the effect of excitation current on the phase transition of the explosive. Experimental research is carried out to verify the feasibility of the emptying method by electromagnetic heating and the effectiveness of the simulation method. The research has significant reference value for electromagnetic heating equipment design and the application of this new method.

2. Basic Principles

The basic principles of emptying explosives with electromagnetic heating can be concisely explained as shown in Figure 1.
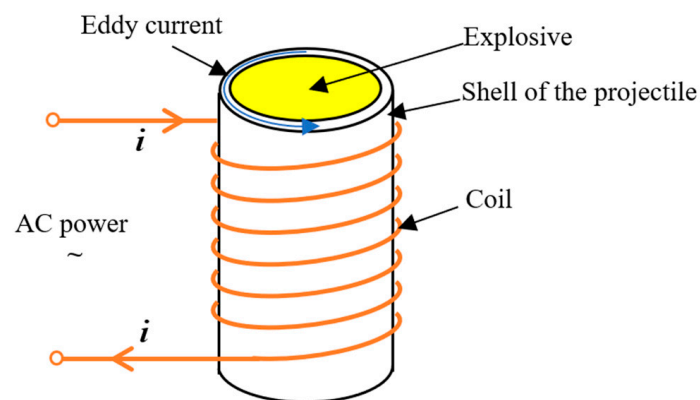

Figure 1. Schematic diagram of emptying explosives with electromagnetic heating.

The inner space of the coil will be filled with a changing magnetic field when the coil is excited by alternating current. According to Faraday's law, an eddy current will be induced in the metallic shell of the projectile under a changing magnetic field, thus forming a heat source. The heat energy will be transferred to the explosive, which is continuously heated and melted. Finally, the melted explosive can be emptied easily.

3. Finite Element Model and Simulation Parameters

To simplify the analysis, the projectile and coil are considered as a two-dimensional axisymmetric model, as shown in Figure 2a. The projectile is date-core-shaped with a maximum radius of 60 mm, a height of 600 mm, and a shell thickness of 5 mm. The minimum radius and height of the bottom are 40 mm and 100 mm, and the minimum radius and height of the opening part are 40 mm and 200 mm. A copper wire coil is wound with 1000 turns and has the same central axis as the projectile. The mesh model for finite element analysis is shown in Figure 2b. Space around the projectile and coil is set to air.
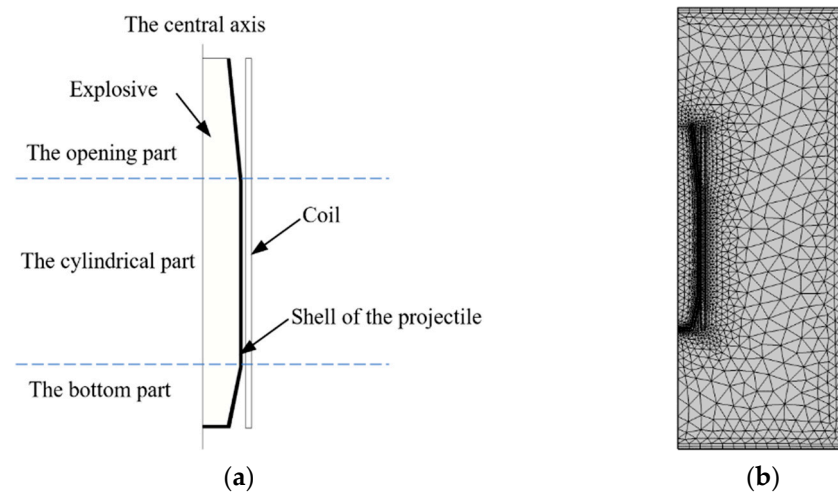
Figure 2. Model for numerical simulation. (**a**) Schematic diagram of the structure. (**b**) Mesh model.

The explosive in the projectile is TNT, the projectile shell is made of carbon steel, and the coil is made of copper. All are placed in air. The material properties are shown in Tables 1–4.

Table 1. The material properties of TNT.

Melting Point (K)	Melt Heating(kJ·kg^{-1})	Heat Capacity (J·kg^{-1}·K^{-1})	Kinetic Viscosity (kg·m^{-1}·s^{-1})	Density of Solid (kg·m^{-3})
353.9	98.45	1610	0.0022	1510

Density of liquid (kg·m^{-3})	Relative permeability	Thermal conductivity of solid (W·m^{-1}·K^{-1})		Thermal conductivity of liquid (W·m^{-1}·K^{-1})
1440	1	0.4		0.35

Table 2. The material properties of carbon steel.

Density (kg·m^{-3})	Relative Permeability	Electrical Conductivity (S·m^{-1})
7870	200	1.12×10^7
Thermal conductivity (W·m^{-1}·K^{-1})		**Heat capacity (J·kg^{-1}·K^{-1})**
76.2		440

Table 3. The material properties of copper.

Density (kg·m^{-3})	Relative Permeability	Electrical Conductivity (S·m^{-1})
8940	1	6×10^7
Thermal conductivity (W·m^{-1}·K^{-1})		**Heat capacity (J·kg^{-1}·K^{-1})**
400		385

Table 4. The material properties of air.

Density (kg·m^{-3})	Relative Permeability	Electrical Conductivity (S·m^{-1})
1.29	1	0
Thermal conductivity (W·m^{-1}·K^{-1})		**Heat capacity (J·kg^{-1}·K^{-1})**
0.0267		1003

As it was difficult to get energetic materials such as TNT, paraffin was used in the experiments to verify the effectiveness of the simulation method. The material parameters

of paraffin are shown in Table 5. Paraffin is a white mixture of hydrocarbons generally melted at 313.15 K to 326.15 K, and it is a poor conductor of electricity, similar to TNT. The performance parameters of paraffin materials are shown in Table 5.

Table 5. The material properties of paraffin.

Melting Point /K	Melting Heat/(kJ·kg^{-1})	Heat Capacity /(J·kg^{-1}·K^{-1})	Kinetic Viscosity /(kg·m^{-1}·s^{-1})	Density (s) /(kg·m^{-3})
313.15~326.16	250.6	2130	0.00689	910

Density (l) /(kg·m^{-3})	Thermal conductivity (s) /(W·m^{-1}·K^{-1})	Thermal conductivity (l) /(W·m^{-1}·K^{-1})	Relative permeability
880	0.3	0.22	1

4. Governing Equations and Boundary Conditions

4.1. Electromagnetic Fields

Electromagnetics phenomena during explosives emptying with electromagnetic heating can be described by Maxwell's Equations, as shown below.

$$\begin{cases} \nabla \times H = J + \frac{\partial D}{\partial t} \\ \nabla \times E = -\frac{\partial B}{\partial t} \\ \nabla \cdot D = \rho_Q \\ \nabla \cdot B = 0 \end{cases} \tag{1}$$

where

H—refers to the magnetic field strength, A/m;
J—refers to the current density, A/m^2;
D—refers to the electrical displacement vector, C/m^2;
E—refers to the electric field strength, V/m;
ρ_Q—refers to the electric charge density, C/m;
B—refers to the magnetic flux density, T;
t—refers to the time, s.

The magnetic vector potential A is introduced for quicker and easier numerical calculations. The electromagnetic field is formed as the time-harmonic form considering the high-frequency alternating form of excitation current. Therefore, Maxwell Equation (1) can be expressed as follows:

$$\begin{cases} \nabla \times H = J + j\omega D \\ E = -j\omega A \\ \nabla \cdot D = \rho_Q \\ B = \nabla \times A \end{cases} \tag{2}$$

where

A—refers to the magnetic vector potential, Wb/m;
ω—refers to the angle frequency, rad/s;

To accurately characterize the distribution of electromagnetic fields, three constitutive equations need to be introduced as follows:

$$\begin{cases} B = \mu H \\ D = \varepsilon E \\ J = \sigma E \end{cases} \tag{3}$$

where

μ—refers to the magnetic permeability, H/m;
ε—refers to the dielectric constant, F/m;
σ—refers to the electrical conductivity, S/m.

Since the magnetic flux density at the boundary of the air domain is small, the tangential component of the magnetic potential is approximately set to zero, so the equation at the boundary can be expressed as follows:

$$\nabla \times A = 0 \tag{4}$$

4.2. Thermal Field

Since the thermal radiation is relatively small, the simulation is approximately conducted regardless of the thermal radiation outside, so the governing equations for thermal analysis can be expressed as follows:

$$\begin{cases} \rho c_p \frac{\partial T}{\partial t} + \rho c_p u \cdot \nabla T + \nabla \cdot q = Q \\ q = -k\nabla T \end{cases} \tag{5}$$

where

ρ—refers to the material density, kg/m^3;
c_p—refers to the constant pressure heat capacity, J/(kg·K);
T—refers to the temperature, K;
u—refers to the speed, m/s;
q—refers to the heat flux, W/m^2;
Q—refers to the heat source, W/m^3;
k—refers to the thermal conductivity, W·m^{-1}·K^{-1};

In this paper, the enthalpy method of porosity is used to simulate the melting process of the explosive, which treats the explosive as a porous area; the porosity of each simulation unit is characterized by the liquid phase rate. The liquid phase rate increases from 0 to 1 while the solid explosive gradually transforms into liquid. The material properties of the explosive in the solid–liquid phase transition stage are calculated with the following equations:

$$\begin{cases} \rho = \theta_1\rho_1 + \theta_2\rho_2 \\ c_\rho = \frac{1}{p}(\theta_1\rho_1 c_{p1} + \theta_2\rho_2 c_{p2}) + L_{12}\frac{\partial \alpha_m}{\partial T} \\ \alpha_m = \frac{1}{2}\frac{\theta_2\rho_2 - \theta_1\rho_1}{\theta_2\rho_2 + \theta_1\rho_1} \\ k = \theta_1 k_1 + \theta_2 k_2 \\ 1 = \theta_2 + \theta_1 \end{cases} \tag{6}$$

where

θ_1, θ_2—refer to the solid phase rate and the liquid phase rate;
ρ_1, ρ_2—refer to the density in solid phase and liquid phase, kJ·m^{-3};
c_{p1}, c_{p2}—refer to the constant pressure heat capacity in solid phase and liquid phase, kJ·m^{-3};
L_{12}—refers to the melting heat, J·kg^{-1}.

The initial temperature is 293.15 K. Since the temperature at the air domain boundary is relatively low, the air domain boundary is set as the thermal insulation condition as follows:

$$-n \cdot q = 0 \tag{7}$$

4.3. Fluid Dynamics Equations

To simplify the calculation, several assumptions are made ignoring the effect of pressure on the density of the explosive. The liquid explosive is approximately considered as a Newtonian incompressible fluid, which flows in the form of unstable laminar flow, so the flow equations can be expressed as follows:

$$\begin{cases} \rho\frac{\partial u}{\partial t} + \rho(u \cdot \nabla)u = \nabla \cdot \left[-pI + u\left(\nabla u + (\nabla u)^T\right)\right] + F + \rho g \\ \rho\nabla \cdot u = 0 \end{cases} \tag{8}$$

where

F—refers to the force per unit volume except for gravity, N/m^3;

p—refers to the pressure, N/m^2;

g—refers to the gravity acceleration, m/s^2;

The explosive density changes with the temperature increase, so the rising force is generated in the fluid due to uneven density, which is the main external force in the fluid flow process besides gravity. The equations can be described as follows:

$$F = (\rho - \rho_{ref})g\alpha(T - T_{ref}) \tag{9}$$

where

ρ_{ref} —refers to the initial density, kg/m^3;

T_{ref}—refers to the initial temperature, K.

The boundary of the explosive satisfies the following equation:

$$u = 0 \tag{10}$$

5. Experimental Research

In order to verify the feasibility of emptying method by electromagnetic heating and the effectiveness of the simulation method, experimental research was carried out. As it was difficult to get energetic materials such as TNT, paraffin was used in the experiments, which has similar physical properties to TNT.

As shown in Figure 3, an experimental system based on the electromagnetic heating method was developed. Figure 3a shows the electromagnetic heater which is composed of four sets of coils, and the four sets of coils can heat the explosives in projectiles independently through high-frequency alternating current. Figure 3b shows the control system of the electromagnetic heater, by which the amplitude and frequency of excitation currents can be set.
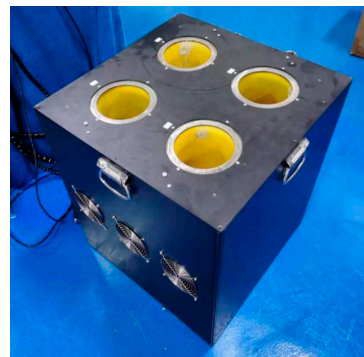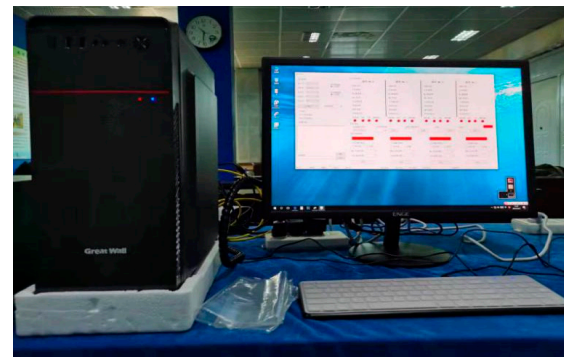
| (a) | (b) |

Figure 3. The experimental system based on the electromagnetic heating method. (**a**) The electromagnetic heater. (**b**) The control system.

A projectile shell-like structure with steel was made, and the paraffin was slowly poured into it. The filling volume of the paraffin is shown in Figure 4a, which can be clearly seen in Figure 4b. This structure was put into one of the coils of the electromagnetic heater. Under a certain excitation current, the paraffin is heated and, finally, melted, as shown in Figure 4c.

Based on the material properties of paraffin and the actual filling volume, a simulation and experiment were carried out. The results under different excitation current parameters are shown in Table 6.
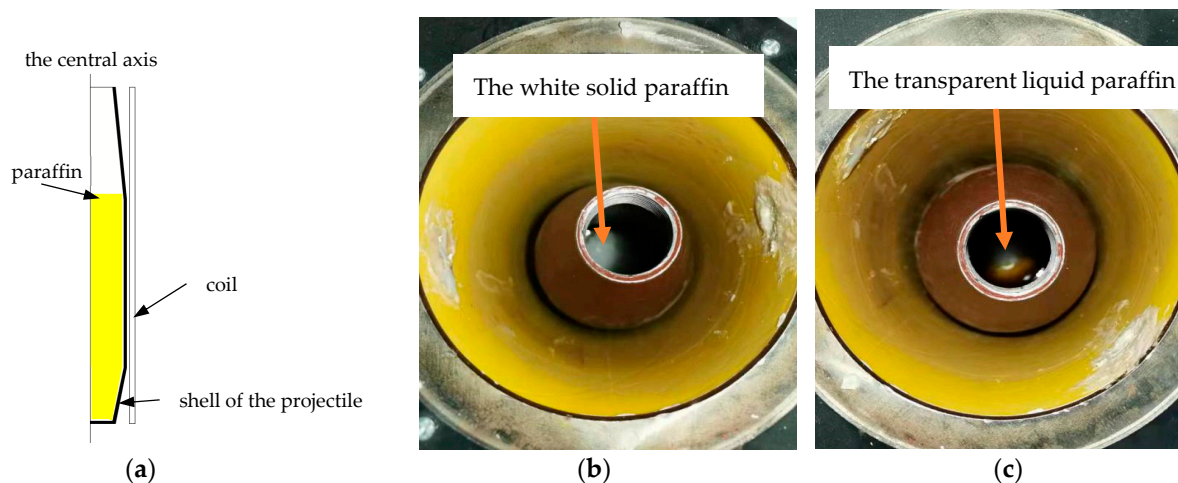
Figure 4. The paraffin state in the projectile shell at different times. (**a**) The filling volume of the paraffin. (**b**) The solid paraffin. (**c**) The melted paraffin.

Table 6. The melting time under different excitation current.

Current Characteristics	1.5 A-10 kHz	2.0 A-10 kHz	2.5 A-10 kHz	2.0 A-5 kHz	2.0 A-15 kHz
The melting time by simulation/min	44	38	29	42	33
The melting time by experiment/min	42	36	28	40	31

Table 6 shows that under different excitation currents, the simulation results and experimental results are basically consistent. Given that the paraffin melting state is mainly obtained through observation, it is difficult to accurately define the time to reach complete melting, and there is a certain deviation between the simulation parameters and the actual parameters, so the melting time by experiment is slightly shorter than the simulation results.

Experimental research shows the simulation method of melting materials with electromagnetic heating is effective, and it also proves that the feasibility of emptying explosives in projectiles by electromagnetic heating.

6. Simulation Results

6.1. Electromagnetic Distribution and Formation of Electromagnetic Heat

The explosive emptying process by electromagnetic heating is simulated with an excitation current magnitude of 2 A and a frequency of 10 kHz. The distribution of the electromagnetic field and the electromagnetic heat are shown in Figure 5.

Figure 5a shows that magnetic field lines are relatively concentrated between the coil and the projectile, which means the magnetic field is mainly distributed in this part, as shown in Figure 5b,c. The maximum magnetic flux density in the space is 0.49 T, which appears at the outer surface of the projectile, but it is only 5.28×10^{-3} T in the explosive, which appears at the edge of the upper opening part. In addition, the maximum electric field strength is 0.759 V/m, which also appears at the edge of the upper opening part, as shown in Figure 5d.

With the effect of the alternating magnetic field, the eddy current is generated at the outer surface of the projectile, and the maximum eddy current density is 4.57×10^7 A/m^2. However, it is almost 0 at the inner surface, as shown in Figure 5e.
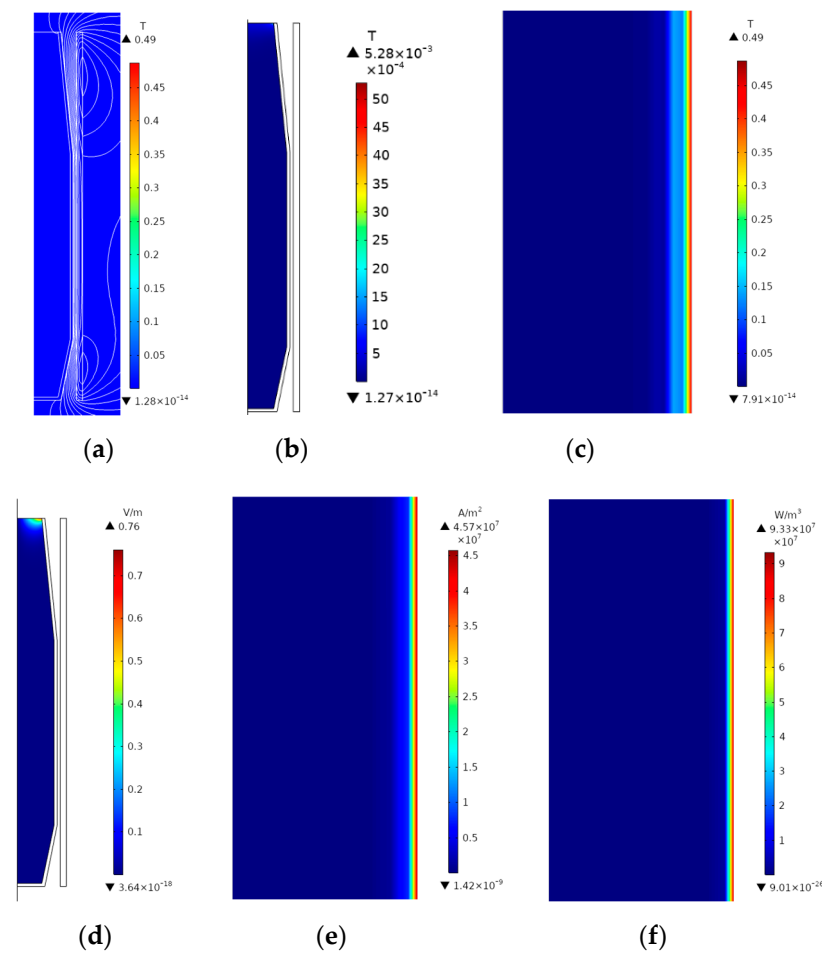
Figure 5. Electromagnetic distribution and formation of electromagnetic heat. (**a**) Magnetic flux density. (**b**) Magnetic flux density in the explosive. (**c**) Magnetic flux density at the shell. (**d**) Electric field intensity in the explosive. (**e**) Eddy current at the shell. (**f**) Power density at the shell.

The skin depth can be estimated according to the equation as follows:

$$\delta = \sqrt{\frac{1}{\pi f u \sigma}} \tag{11}$$

where

　　δ—refers to the skin depth, m;

　　f—refers to the frequency, Hz.

　　μ—refers to the magnetic permeability, H/m;

　　σ—refers to the electrical conductivity, S/m.

　　The skin depth at the shell is only 0.11 mm, approximately, while the frequency of excitation current is 10 kHz. The distribution of the electromagnetic field indicates that the metal shell of the projectile acts as an excellent electromagnetic shielding shell for the explosive during the emptying process.

　　A heat source is created as there exists an eddy current. According to Joule's Law, Ohm heat is proportional to the square of the current. Therefore, the heat power density reduces gradually from the outside to the inside. The maximum power density is 9.33×10^7 W/m^3, but it is almost 0 at the inner surface, as shown in Figure 5f. The total heating power can be calculated by a volume integral, which is 913.55 W under this condition.

　　To analyze the effect of excitation current characteristics on the electromagnetic field and the electromagnetic heat, the excitation current amplitude is set to 1.5 A, 1.75 A, 2.25 A

and 2.5 A, and the frequency is set to 5 kHz, 7.5 kHz, 12.5 kHz and 15 kHz, respectively. The results are shown in Figure 6.
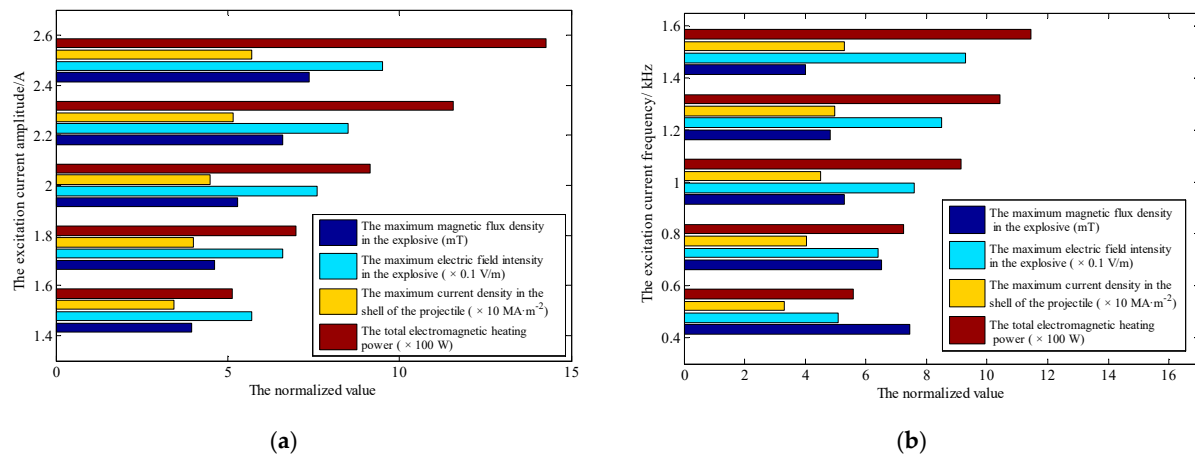

(**a**)   (**b**)

Figure 6. The effect of excitation current characteristics on the electromagnetic field and the electromagnetic heat. (**a**) Simulation results with different current amplitude. (**b**) Simulation results with different current frequency.

According to Figure 6, it can be concluded that the electric field intensity in the explosive, the current density in the shell of the projectile and the electromagnetic heating power will be all enhanced with the excitation current amplitude and frequency increasing. However, the magnetic flux density in the explosive decreases as the excitation current frequency increases, for the electromagnetic shielding effect of the projectile shell is more obvious when the alternating magnetic field changes more quickly.

6.2. Temperature Distribution and Phase Change

The temperature and liquid rate distribution in the explosive are shown in Figures 7 and 8, with the excitation current amplitude of 2 A and the frequency of 10 kHz. At the initial stage, the temperature is 293 K, and the explosive is completely in a solid phase. With the explosive heated continuously, the temperature rises. The maximum temperature reaches 357 K, and the explosive near the projectile begins to melt at 8 min, as shown in Figures 7b and 8b. The distribution of temperature and liquid rates at 10 min, 30 min and 50 min are shown in Figures 7c–f and 8c–f, respectively. Due to electromagnetic heating, the temperature rises continuously. In the explosive, the heat energy is conducted from the edge to the inside, increasing the proportion of the liquid phase. In addition, due to the density difference, the liquid explosive moves up, and the solid explosive sinks with the effect of volume force. The liquid explosive is mainly distributed in the upper part of the projectile. At 52 min, the minimum temperature has exceeded the melting point of the explosive of 353.9 K. Therefore, the explosive melts thoroughly, as shown in Figures 7f and 8f.
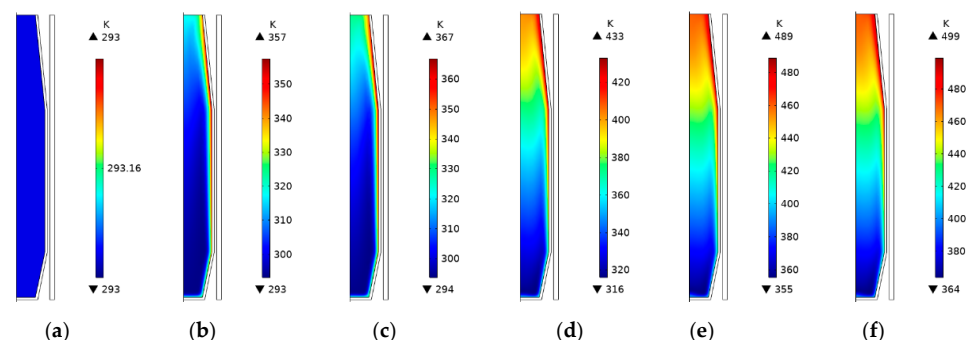

(**a**)   (**b**)   (**c**)   (**d**)   (**e**)   (**f**)

Figure 7. Temperature distribution of the explosive. (**a**) 0 min. (**b**) 8 min. (**c**) 10 min. (**d**) 30 min. (**e**) 50 min. (**f**) 52 min.
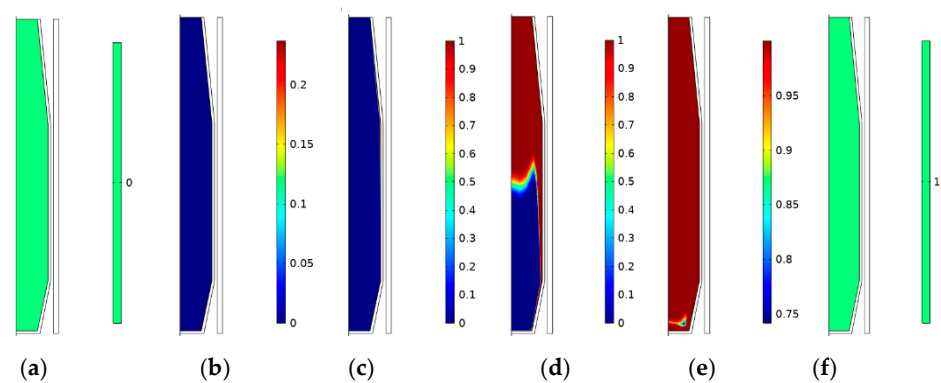
Figure 8. Phase change of the explosive. (**a**) 0 min. (**b**) 8 min. (**c**) 10 min. (**d**) 30 min. (**e**) 50 min. (**f**) 52 min.

6.3. The Influence of Excitation Current Characteristics on The Melting Process

To study the influence of the frequency on the melting process, the excitation current amplitude is kept at 2 A. The maximum temperature and the proportion of the liquid phase with time are shown in Figure 9a,b under the condition that the excitation current frequency is 5 kHz, 10 kHz and 15 kHz, respectively.
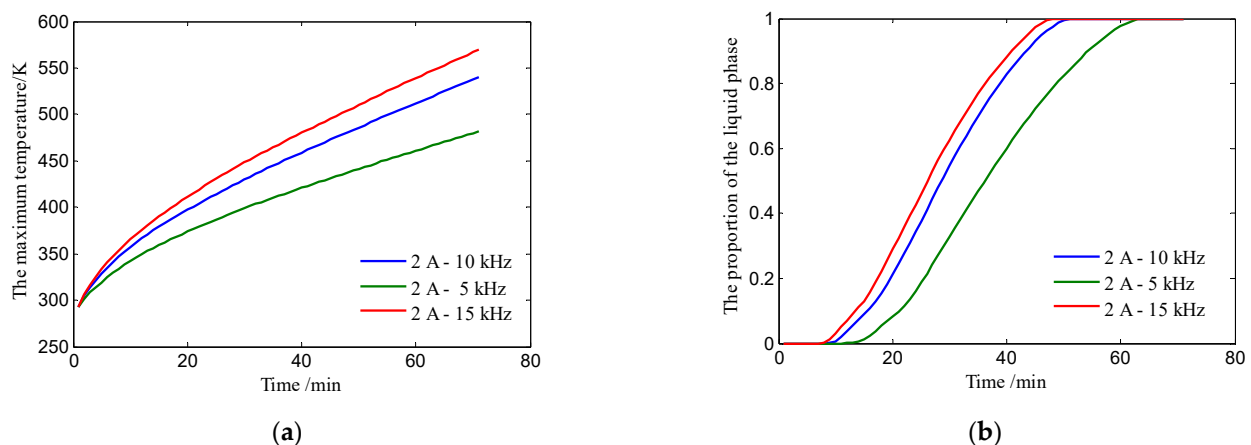

Figure 9. The performance with different current frequency. (**a**) The maximum temperature in the explosive. (**b**) The proportion of the liquid phase.

The maximum temperature in the explosive with time in Figure 9a illustrates that the higher the excitation current frequency, the faster the temperature rise. In addition, Figure 9b shows that the explosive begins to melt at 11 min, and wholly melts at 64 min when the excitation current frequency is 5 kHz. The two moments are 8 min and 52 min with the excitation current frequency of 10 kHz, which are 7 min and 50 min with the excitation current frequency of 15 kHz. The duration times of the melting process are 53 min, 44 min and 43 min, respectively. It can be concluded that with the excitation current frequency increasing, the eddy current effect becomes stronger, and the generated heat power increases, indicating that the heating rate can be controlled by adjusting the excitation current frequency.

For the study on how the excitation current amplitude affects the melting process, the excitation current frequency is kept at 10 kHz. When the excitation current amplitude is set as 1.5 A, 2 A, and 2.5 A, respectively, the maximum temperature and the proportion of the liquid phase with time are shown in Figure 10a,b, accordingly.
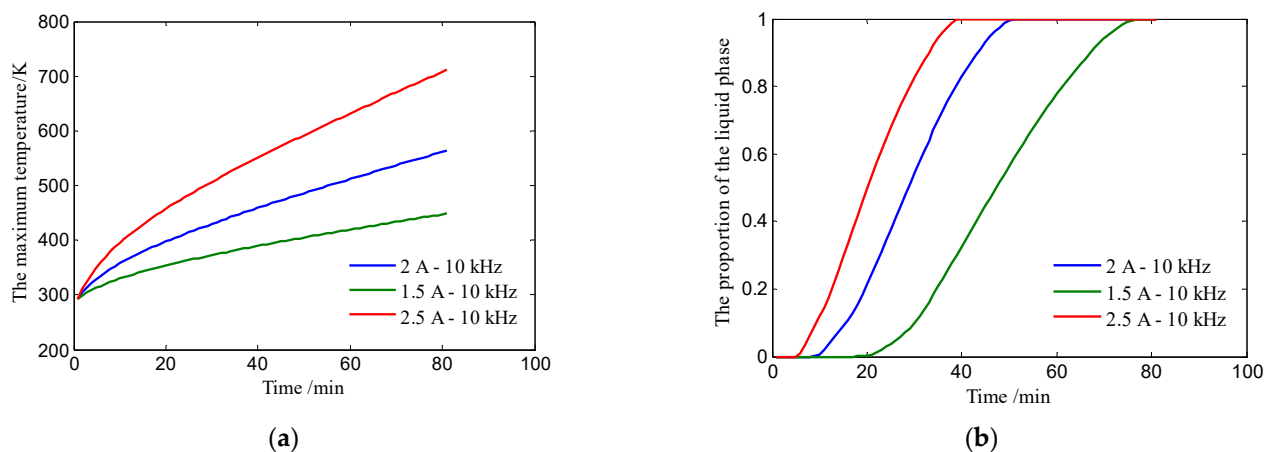
(a)   **(b)**

Figure 10. The performance with different current amplitude. (**a**) The maximum temperature in the explosive. (**b**) The proportion of the liquid phase.

As Figure 10 shows, the larger the excitation current amplitude, the faster the temperature rise. The times that the explosive begins to melt and melts thoroughly are 17 min and 78 min, respectively, when the excitation current amplitude is 1.5 A. The two times are 8 min and 52 min, respectively, with the excitation current amplitude of 2 A, and 5 min and 40 min, respectively, with the excitation current amplitude of 2.5 A. The durations of the melting process are 59 min, 44 min and 35 min, respectively, so the conclusion is that with the excitation current amplitude increasing, the heat generated power increases, indicating that the heating rate can be controlled by adjusting the excitation current amplitude.

7. Conclusions

Emptying explosives in projectiles with electromagnetic heating provides a new method for the disposal of end-life projectiles. In this paper, a multiple physical fields simulation model is developed, the dynamic emptying process is obtained and the effect of the excitation current characteristics on the emptying process is studied. The following can be concluded:

a. Heat is generated in the projectile shell under the altering electromagnetic field, causing the explosive to melt completely. Thus, the feasibility of emptying explosives with electromagnetic heating is verified, which provides an effective method for emptying explosives in end-life projectiles.

b. During the heating process, the explosive near the shell melts first, then the liquid explosive with lower density floats up and the solid explosive with higher density sinks, which means if the projectile is turned upside down, the explosive may all flow out with no need to melt completely. The simulation results provide a reference for the structural optimization of electromagnetic heaters.

c. The excitation current parameters have a significant effect on the explosive heating rate, which indicates that the explosive melting process would be controllable with this method. So, it would be efficient and safe for emptying explosives by setting proper current parameters.

References

1. Yang, Q.X.; Du, B.W.; Xuan, Z.I.; Li, T.P.; Yao, K.; Mu, W.L. Analytical method for main influence factors of ammunition storage environment based on grey correlation entropy. *J. Ordnance Equip. Eng.* **2020**, *41*, 86–89.
2. Li, J.M.; Lei, B.; Ding, Y.K. Emptying Technology for End-of-Life Ammunition. In *Technology of Conventional Ammunition Disposal*; China National Defense Industry Press: Bejing, China, 2012.
3. Tong, Y.; Liu, Y.; Huang, F.L. Research advancement of current destructive technology for outdated ammunitions. *J. Saf. Environ.* **2020**, *20*, 1910–1923.
4. Yoh, J.J.; McClelland, M.A.; Maienschein, J.L.; Wardell, J.F. Towards a predictive thermal explosion model for energetic materials. *J. Comput. -Aided Mater. Des.* **2005**, *10*, 175–189. [CrossRef]
5. Jia, S.Z.; Zhen, J.W.; Sun, F.B.; Liu, D.D.; Xue, T.; Hu, Z.Y. Analysis and application of safety combustion model of unexploded ordnance. *New Chem. Mater.* **2021**, *49*, 158–161, 166.
6. Zhao, Q.L.; Ye, Z.F.; Zhang, M.H. Treatment of 2,4,6-trinitrotoluene(TNT) red water by vacuum distillation. *Chemosphere* **2010**, *80*, 947–950. [CrossRef] [PubMed]
7. Marinovic, V.; Ristic, M.; Dostanic, M. Dynamic adsorption of trinitrotoluene on granular activated carbon. *J. Hazard. Mater.* **2005**, *117*, 121–128. [CrossRef] [PubMed]
8. Zhu, K.K.; Huang, F.; Zhang, X.Y.; Deng, C.C.; Chen, L.; Wang, Z. Study status destroying used projectile. *Anhui Chem. Ind.* **2021**, *47*, 11–12, 16.
9. Xia, F.J.; Song, G.F.; Xiao, D.S.; Wang, S. Research on development thoughts of green harmless disposal technology for condemned ammunition. *Ordnance Ind. Autom.* **2011**, *30*, 94–96.
10. Xiang, H.J.; Lei, B.; Xing, Y.C. Analysis and design on technology of emptying explosive from pellet by EM-induction heating. *J. Proj. Rocket. Missiles Guid.* **2015**, *35*, 47–50.
11. Chen, Z.X.; Zheng, D.; Wang, J.; Chen, L.; Sundén, B. Experimental investigation on heat transfer characteristics of various nanofluids in an indoor electric heater. *Renew. Energy* **2020**, *147*, 1011–1018. [CrossRef]
12. Wang, J.; Li, G.L.; Li, T.; Zeng, M.; Sundén, B. Effect of various surfactants on stability and thermophysical properties of nanofluids. *J. Therm. Anal. Calorim.* **2021**, *143*, 4057–4070. [CrossRef]
13. Zhang, Y.L.; Zhang, X.M.; Wu, Y.T.; Lu, Y.; Ma, C. Analysis of thermal performance of electromagnetic induction based molten salt heating system. *Energy Storage Sci. Technol.* **2019**, *8*, 319–325.
14. Zhang, Y.Y.; Chen, B.M.; Li, J.Y.; Zhang, Z.S. Study on the influence of porous skeleton on solid-liquid phase change based on pore size. *J. Shandong Jianzhu Univ.* **2019**, *34*, 56–62.
15. Cai, W.C.; Yang, W.; Zhang, B.K.; Fan, J.H.; Wu, J.Y.; Xing, T.; He, R. A combined numerical and experimental study on melting process of paraffin phase change. *J. Southwest Univ. Sci. Technol.* **2018**, *33*, 6–9, 81.
16. Cheng, S.Y.; Chen, B.M.; Guo, M.X.; Zhang, Y.Y.; Li, J.Y. Effect of fin arrangement on melting of phase change material in rectangular cavity. *Gas and Heat* **2020**, *40*, 7–12, 15.
17. Guo, M.X. Influence of Inner Tube Arrangement and Wall Temperature of Casing-type Phase-change Heat Accumulator. *Gas Heat* **2019**, *39*, 1–7.
18. Li, S.H.; Guan, X.C.; Lei, B.; Li, Z. Simulation analysis of the temperature field in an induction Launcher. *IEEE Trans. Plasma Sci.* **2013**, *41*, 1055–1060.
19. Lv, P.Y.; Zhang, X.H. Numerical research on the effect of frequency on induction heating in electromagnetic cold crucible. *J. Northeast. Electr. Power Univ.* **2019**, *39*, 72–79.
20. Fu, Y.M.; Zheng, L.J.; Li, Y.F. Development of crack arrest by using electromagnetic heating and its applications on welding joint strengthening. *China Mech. Eng.* **2014**, *25*, 1828–1837.